INSTITUTE OF TECHNOLOGY

AIR UNIVERSITY

UNITED STATES AIR FORCE

SCHOOL OF ENGINEERING

THESIS

WRIGHT-PATTERSON AIR FORCE BASE, OHIO

AF-WP-B-SEP 60 5M

STRAIN AGING
IN MOLYBDENUM

THESIS

Presented to the Faculty of the School of Engineering of
the Institute of Technology
Air University
in Partial Fulfillment of the
Requirements for the Degree of
Master of Science

By
Robert J. Wilson
Major USAF
Graduate Aeronautical Engineering
(Air Weapons Option)
August 1961

Preface

After many months of theoretical study, I have enjoyed the opportunity to conduct some experimental work which gives real results and satisfaction of first-hand knowledge.

The purpose of this study is to provide, by experiment, data on molybdenum not previously obtained. It will add to the total knowledge about refractory metals in general. The investigation concerns the characteristics of strain-aging in molybdenum by using dynamic modulus and yield-point return measurements. It provides an activation energy for interstitial diffusion in commerical-purity molybdenum but does not establish which interstitial element is associated with that energy. The experimental work was done at the Directorate of Materials and Processes.

The author is pleased to acknowledge indebtedness to the following people of the Directorate of Materials and Processes: Lt C. S. Hartley, of the Metals and Ceramics Laboratory, for providing the thesis topic and guidance throughout the investigation; George King, for the use of the dynamic modulus equipment and the accompanying instructions; Lt B. A. Wilcox, for his information and advice on the experimental methods; and all those who were quick to help and furnish equipment.

The author also wishes to thank Capt E. J. Myers, his thesis advisor, for helpful suggestions and comments and aid in obtaining reference material; Helen M. Caldwell, Institute library secretary, for obtaining reproductions from a long list of references so he might read them during his stay in the hospital; and finally, his wife, for typing the draft of this report.

Robert J. Wilson

Contents

List of Figures

List of Tables

Abstract

The purpose of the investigation was to study the characteristics of strain aging in commercial-purity molybdenum by the methods of dynamic modulus recovery and yield point return, and to determine the activation energy of strain aging.

Modulus specimens, from arc-cast, recrystallized molybdenum, in the shape of rectangular bars were deformed three percent in compression. The return of Young's modulus was investigated as a function of aging time and temperature using a free-free beam method of flexural vibration. Measurements of resonant frequency were made at room temperature. For convenience, the rate of increase of the square of resonant frequency, rather than modulus recovery was used to plot the data for determining an activation energy. The logarithm of the rate of increase was plotted versus the reciprocal of the absolute temperature. The slope of the straight line drawn through the points represented the activation energy for the process of strain aging.

Tensile specimens from powder-metallurgy molybdenum sheet, 0.008 inch thick, were given approximately two percent plastic deformation by straining to the end of the lower yield stress. The rate of return of yield point with aging time and temperature was plotted as above to give an activation energy. The tensile testing was done at room temperature using an Instron machine.

The aging was done in a molten mixture of Wood's metal and tin set in a pot furnace. Close temperature control was obtained by using a variac-controlled, constant voltage transformer.

The rate of Young's modulus recovery gave values of activation energy from 24,000 to 28,000 calories per mole. The rate of yield point return gave a single value of 24,000 calories per mole. The upper limiting temperatures for reliable data on the strain aging process was found to be approximately 300°C for modulus recovery and 580°C for yield point return. The interstitial element responsible for strain aging was narrowed down to a choice between carbon and oxygen.

STRAIN AGING
IN MOLYBDENUM

I. Introduction

The investigation was conducted to study the characteristics of strain aging in commercial-purity molybdenum and to determine the activation energy of strain aging. The significance of the investigation is to provide experimental data which have not been obtained previously on molybdenum. It furnishes information on the mechanical behavior of molybdenum and adds to the total information on refractory metals in general.

Background

In recent years, the developments in jet, rocket, and nuclear engines, missiles and space vehicles have created a demand for materials able to withstand high loads at high temperatures. Molybdenum, a group VIa metal in the periodic table of elements, belongs in the class of body-centered cubic refractory metals which show promise as suitable materials for these high temperature structural applications.

Molybdenum has the atomic number 42 and atomic weight 95.95. Its electron configuration, (2) (8) (18) (2s, 6p, 5d) (1s) typifies it as a transition element. The 5 unpaired 4d electrons account for its high strength, modulus of elasticity, and melting point (Ref 13:31).

Before proceeding further, some of the terms used throughout the paper will be defined. The body-centered cubic structure of a polycrystalline metal has an atom at each corner of a basic cube and one in the center of the cube-body. Sometimes, very small amounts of the elements carbon, hydrogen, nitrogen, oxygen, and boron occupy the spaces or interstices throughout the cubic structure. For this reason they are called interstitial elements. Carbon, nitrogen, and oxygen are the elements typically found in molybdenum.

In strain aging, the interstitial solute atoms interact with dislocations. Dislocations are line defects in the crystal structure and, for the purpose here, can be considered as a missing line of atoms in the crystal lattice. A typical dislocation density in annealed metals is 10^8 lines per square centimeter (Ref 4:112).

A unit cell of the body-centered cubic structure is shown in Figure 1(a). The dots represent the possible positions of 1/2 0 0 and 1/2 1/2 0 occupied by the interstitial atoms (Ref 3:895). Figure 1(b) shows what the structure might look like in the region of a dislocation.

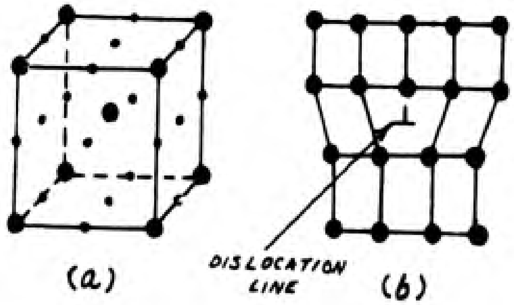

FIG. 1
(a) b.c.c. STRUCTURE
(b) DISLOCATION LINE

Theory

Briefly, strain aging is caused by the migration of the interstitial solute atoms back to the sites surrounding dislocations which have been separated from the pinning atoms by plastic deformation. It is a metallurgical change which affects the mechanical behavior of the metal and produces a strengthening effect (Ref 8:361).

The mechanism of strain aging can be explained by the widely accepted Cottrell theory of dislocation-solute atom interaction

(Ref 2:30-37). According to the theory, the solute atoms tend to take up positions in the regions of dislocations. When formed in an atmosphere surrounding dislocations, the solute atoms are in their most stable or lowest energy positions and have the effect of pinning the dislocations to prevent their movement in the lattice. If a metal with this internal structure is deformed by a high enough stress, either tensile or compressive, the dislocations will be torn free of the pinning atoms. With sufficient temperature and time the aging process will occur.

Strain aging is a rate process conforming to the semi-empirical relation

$$\text{Rate of reaction} = A \exp(-Q/RT)$$

Where A is a frequency factor,

Q is the activation energy per mole, or the smallest energy necessary for the process to begin,

R is the universal gas constant in calories per mole degree,

and T is the absolute temperature.

By expressing the reaction rate as the reciprocal of the time to reach a selected stage in the process, and taking the natural logarithm of both sides of the equation, the relation is shown as:

$$\ln\left(\frac{1}{t}\right) = \ln A - Q/RT$$

This shows that the logarithm of the process rate should vary linearly with the reciprocal of the absolute temperature. If $\ln\left(\frac{1}{t}\right)$ is plotted against $\frac{1}{RT}$, as shown in Figure 2, the slope of a straight line drawn through the points gives the value of the activation energy, Q.

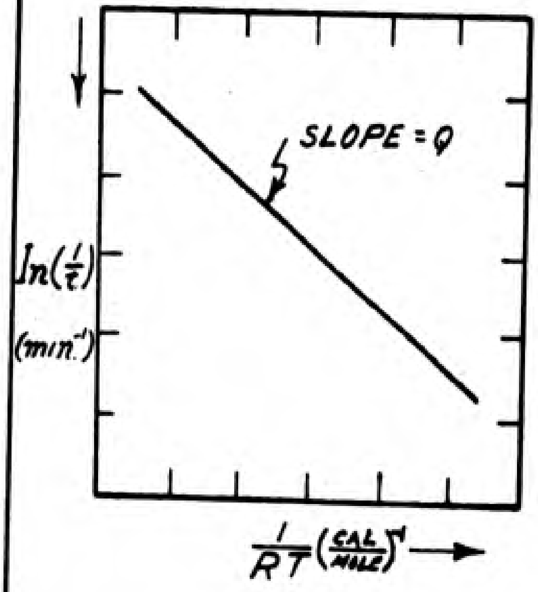

FIG. 2

PLOT FOR ACTIVATION ENERGY (Q)

Previous Work

A previous investigation of strain-aging in high-purity molybdenum wire was conducted by Maringer and Schwope (Ref 9:24-33). They found that changing the content of oxygen and nitrogen did not affect the strain aging characteristics. A change in aging behavior did occur after carbon removal, and it was concluded that carbon atoms interacting with dislocations caused the strain-aging. Maringer and Schwope reported an activation energy of 15,600 calories per mole.

Strain aging in body-centered cubic iron has been widely investigated. A method commonly used to study the process of strain aging in iron is the measurement of yield point return. Another technique, developed by Lt B. A. Wilcox of the Directorate of Materials and Processes, is the measurement of dynamic modulus to determine the rate of modulus recovery caused by strain aging. He used these methods with good success to investigate dislocation locking in niobium, and found good agreement between the activation energies for strain aging by each method. Comparing the value of activation energy for strain aging with that reported for interstitial diffusion by other experimenters, he was able to conclude that hydrogen was responsible for strain aging in niobium (Ref 14:292-303).

Following the example of Wilcox, the strain aging behavior of molybdenum has been investigated by two methods:

1. Dynamic modulus measurements to determine the rate of modulus recovery.

2. Return of yield point measurements to determine the rate of yield point return.

II. Dynamic Modulus Measurements

Dynamic methods for determining Young's modulus of elasticity, E = normal stress/normal strain, have become more popular than the usual method of applying a stress and recording the resultant strain. These methods are nondestructive and generally more precise. The specimen is vibrated by various techniques and its resonant frequency measured. Knowing this frequency, E can be calculated. Examples of dynamic tests to determine E are: longitudinal vibration, which requires an ultrasonic oscillator to vibrate the specimen in the length direction; and flexural bending, which includes various techniques for vibrating the specimen and supporting its ends (Ref 11:84-87).

In this study, a free-free beam method of flexural bending was used to obtain the resonant frequency of molybdenum bars in the shape of rectangular parallelepipeds. The nominal dimensions of the bars were: length, 4 inches; width, 0.5 inch; and thickness, 0.25 inch. The modulus was calculated using the relation

$$E = 0.94645 \frac{C\, m\, f^2}{B} \qquad \text{(Ref 5:8)}$$

where E is Young's modulus in dynes per cm^2

0.94645 is a factor for converting from English to CGS units

C is a shape factor

m is the mass in grams

f is the resonant frequency of the fundamental mode of flexural vibration, in cycles per second.

B is the dimension width of the cross-section perpendicular to the direction of the vibration, in centimeters.

Figure 3 shows the rectangular specimen with its dimensions labeled.

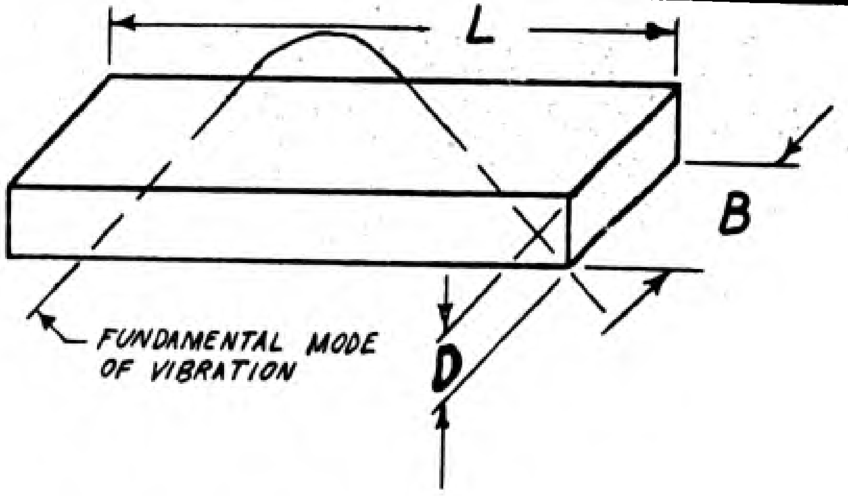

FIG. 3

MODULUS SPECIMEN

Tables of the shape factor C have been compiled for various values of D/L and Poisson's ratio (Ref 5:147). The value of Poisson's ratio (u) was assumed to be 0.30.

<u>Sample Calculation</u>

$$(E = 0.94645 \frac{C\,m\,f^2}{B})$$

Specimen #3

assume u = 0.30

L = 3.999 inches

B = 0.4845 "

$\frac{D}{L} = \frac{0.2485}{3.999} = 0.0621$

D = 0.2485 "

f = 3503 c/s

m = 80.4892 gms

From the table for $u = 0.30$ and $\frac{D}{L} = 0.0621$ the shape factor

$$C = 4291.15$$

$$E = \frac{(0.94645)(4291.15)(80.4892)(3503)^2}{(0.4845)(2.54)}$$

$$E = 3.26896 \times 10^{12} \text{ dynes/cm}^2$$

To convert to pounds per square inch multiply by the factor

$$\frac{6.4516 \text{ cm}^2/\text{in.}^2}{444,820 \text{ dynes/lb}} = 1.4504 \times 10^{-5} \frac{\text{cm}^2 \text{ lb}}{\text{dyne in.}^2}$$

$$E = 47.276 \times 10^6 \text{ psi}$$

Specimen History

The material for the modulus specimens were donated by the General Electric Research Laboratory, Schnectady, New York. Better than commercial purity, the metal was arc cast, extruded with a ten to one ratio at 1650°C (3000°F), and forged 50 percent at 1316°C (2400°F) by the G. E. Laboratory. The Metals and Ceramics Laboratory cut the metal specimens and recrystallized them in a vacuum annealing furnace for one hour at 1316°C (2400°F).

Description of Modulus Equipment

A block diagram of the equipment used to measure resonant frequency of the specimen is shown in Figure 4. A photograph of the setup is shown in Figure 5.

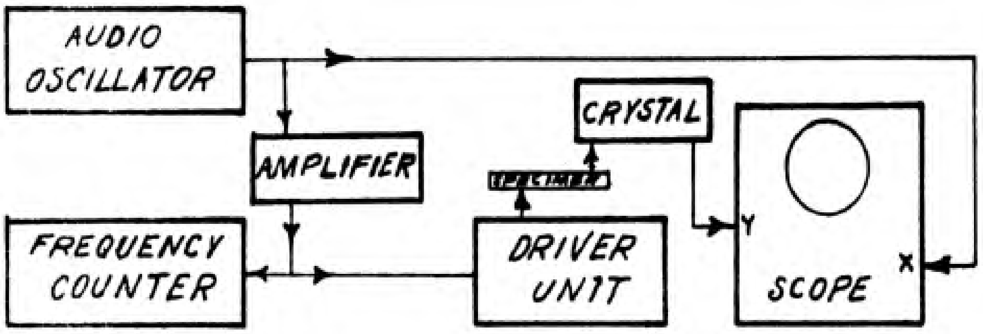

FIG. 4

BLOCK DIAGRAM OF EQUIPMENT FOR MEASURING RESONANT FREQUENCY

Equipment:

Audio Oscillator;	Hewlett Packard, model 201C, 0-20,000 c/s
Amplifier;	Masco, model MA-BN
Frequency Counter;	Berkely, model 554A
Driver Unit;	Calrad, TS-251, 25W, 16 ohm (public address)
Crystal Amplifier:	Astatic, type 12-u
Oscilloscope;	Tektronix, 545

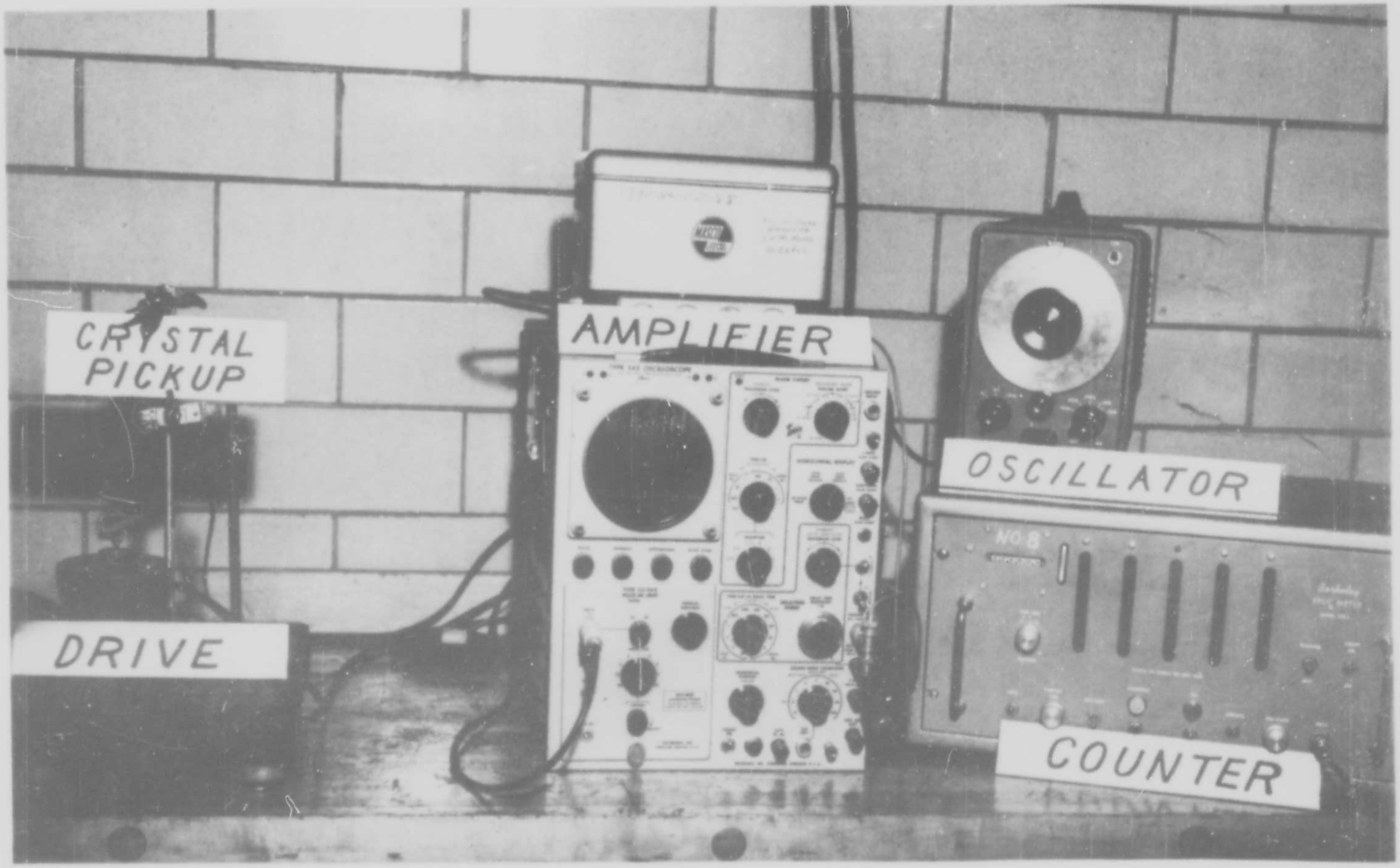

Fig. 5
Apparatus for Determining Young's Modulus from Flexural Vibration

The sequence of events can be described as follows. A frequency signal generated by the audio oscillator is sent to the horizontal deflection plates (X) of the oscilloscope, and also amplified and sent to the frequency counter and driver unit. The driver vibrates the specimen near the nodal point at one end, and a fine wire picks up the response at the other end. (The nodal point has been determined previously to be located at 0.224 of the length based on the free-free end conditions applied to the differential equation for flexural vibration) (Ref 11:54). The response is amplified by a phonograph crystal, and sent to the vertical set of deflection plates (Y). When the frequency ratio of response frequency to input frequency is unity it signifies resonance in the specimen, and is indicated by the appearance of an elliptical Lissajous figure on the scope. The resonant frequency, which can be read to tenths of a cycle, was determined to the nearest cycle after each period of aging.

Description of Aging Equipment

The equipment used for aging was selected to provide a high temperature bath (200°C - 600°C) with close temperature control and rapid heat transfer to the specimen. An air furnace and a silicone oil bath were tried but neither proved satisfactory. By attaching a thermocouple to the specimen, it was found that each method took approximately four minutes to bring the specimen from room temperature to the aging temperature. Because of this, the cumulative aging time could not be determined accurately. A satisfactory solution was found by using a crucible of molten metal set in a pot furnace. The metal bath contained approximately 50 percent tin and 50 percent Wood's metal by weight. The composition of the Wood's metal is:

Constituent	Weight (Percent)
Bismuth	50.7
Lead	25.2
Tin	12.3
Cadmium	11.9

The melting point of Wood's metal is 74.5°C, and that of tin 232°C. The combination gave a molten bath well below the lowest temperature used, 241°C. The heat transfer was checked at 388°C by using a chromel-alumel thermocouple spot welded to a modulus specimen. The specimen reached a temperature of 371°C in ten seconds and 388°C in fifteen seconds. There was no alloying of the specimen and bath metal.

A block diagram of the apparatus used for the aging process is shown in Figure 6. A photograph of the entire arrangement is shown in Figure 7. The Wood's metal and tin were melted down in a higher wattag pot furnace, and then transferred to the smaller furnace shown in Figure 7 for more sensitive temperature control.

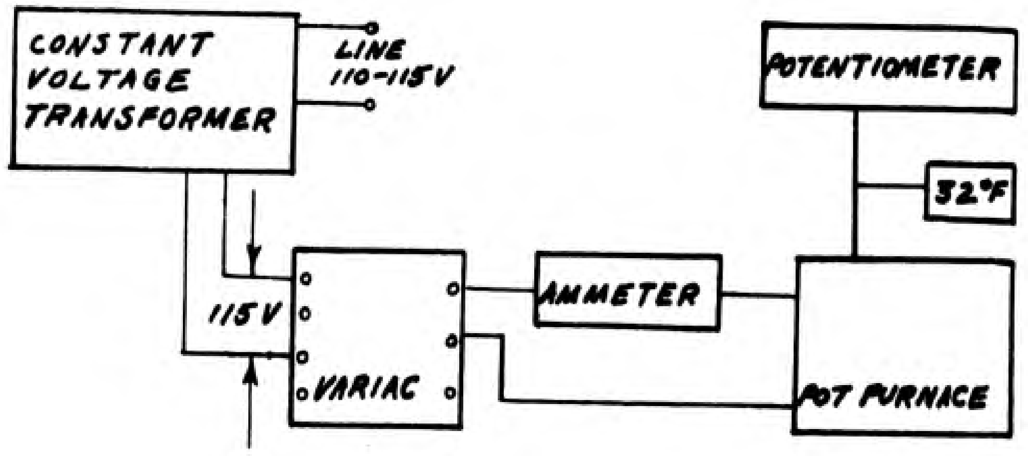

FIG. 6

EQUIPMENT FOR CONTROLLING AGING BATH TEMPERATURE

Equipment:

Transformer;	Sola, 1000 VA, 115V, 8.7A
Furnace;	Hoskins, 110V, 10.9A
Ammeter;	Weston, A.C., model 433, 10V full scale
Potentiometer;	Leeds & Northrup (bridge type)
Thermocouple;	Chromel-Alumel

The equipment in Figure 6 operates as follows. Line voltage is fed to a transformer which has a constant output of 115 volts to the variac for a line variation from 95 to 125 volts. The variac controls the amount of voltage applied to the furnace load. The ammeter is inserted for convenience in calibrating a setting for a desired bath temperature, and to insure against exceeding the amperage limitation of the transform

Temperature monitoring was done by a chromel-alumel thermocouple connected to a bridge-type potentiometer, calibrated in degrees Fahrenheit, with an ice-bath cold junction. The temperature variation of the static molten bath was within one degree Fahrenheit for a 24-hour period.

Procedure

Six specimens were used to obtain data for six aging temperatures from 241°C to 388°C. First, the resonant frequency of the undeformed specimen was measured. Next, the specimen was deformed three perce in compression in a Baldwin-Southwark press (200,000 lb capacity). This required a load of 170,000 pounds (85,000 psi). Immediately after compressing, the deformed sample was tested for resonant frequency to represent zero aging time. It was found that molybdenum showed no measurable aging effect at room temperature, which made it convenient to take all frequency readings at room temperature. After the zero-aging time frequency was recorded, the specimen was placed in the molten

Fig. 7
Aging Bath Apparatus

metal bath for elevated-temperature aging for selected time intervals. At the end of each interval, the specimen was quenched to room temperature and tested for resonant frequency. The return of resonant frequency toward the undeformed value with aging time was recorded for the particular temperature. The most accurate method for obtaining consistent readings of resonant frequency, on the counter, was to switch the horizontal display control of the oscilloscope from external to main sweep, and adjust the frequency of the audio oscillator for maximum amplitude on the oscilloscope. By switching to main sweep, a sine wave was displayed on the scope instead of the Lissajous figure. The sine wave displayed maximum amplitude at the peak of resonant frequency. The maximum amplitude was sharply defined, and could be determined within plus or minus one-tenth of a cycle per second.

Table I lists the six temperatures and the corresponding times to maximum recovery. Appendix A contains a tabulation of the data for six aging temperatures.

Table I

Temperatures and Aging Times
for Modulus Recovery

Temperature	Aging Time to Maximum Recovery
241°C (466°F)	550 minutes
260°C (500°F)	400 "
280°C (536°F)	350 "
299°C (570°F)	330 "
343°C (650°F)	240 "
388°C (730°F)	110 "

The time to maximum recovery had no significance in the determination of activation energy since it did not represent the recovery of the same increment of frequency for each specimen. The table does show that the time to maximum recovery became progressively less as the temperature was increased.

Method For Reporting Data

The primary aim of the investigation was to determine an activation energy for the strain aging process. Values of the modulus, E, could have been plotted to show the recovery of the modulus with aging time and temperature. Since E is proportional to f^2, it was more convenient to plot, in Figure 12, the change in the square of the frequency between a given aging time and zero-aging time versus the logarithm of the aging time. These values of $\Delta(f^2)$ are tabulated along with the raw data in Appendix A.

The time to recover a specific number of cycles at each temperature was determined by passing a horizontal line, representing the value of $\Delta(f^2)$, through the family of curves (see Figure 12, facing page 22). The intersections of the horizontal line and the curves gave the times and temperatures for a plot of $\ln(\frac{1}{t})$ versus $\frac{1}{RT}$. A straight line was drawn through the points of this plot, and its slope was taken as the activation energy for the process.

III. Return of Yield Point Measurements

This part of the investigation was conducted to determine the activation energy for strain aging of molybdenum from the rate of yield point return, and to compare the result with the activation energy obtained by the dynamic modulus method.

When the specimen is subjected to an increasing tensile load, the point at which the dislocations are torn away from the pinning solute atoms is indicated by a sharp yield called the upper yield point. The specimen will continue to deform at a lower value of load (stress) until strain hardening causes the load (stress) to increase. Figure 8 shows parts of interest of the stress-strain, or load-elongation, curve.

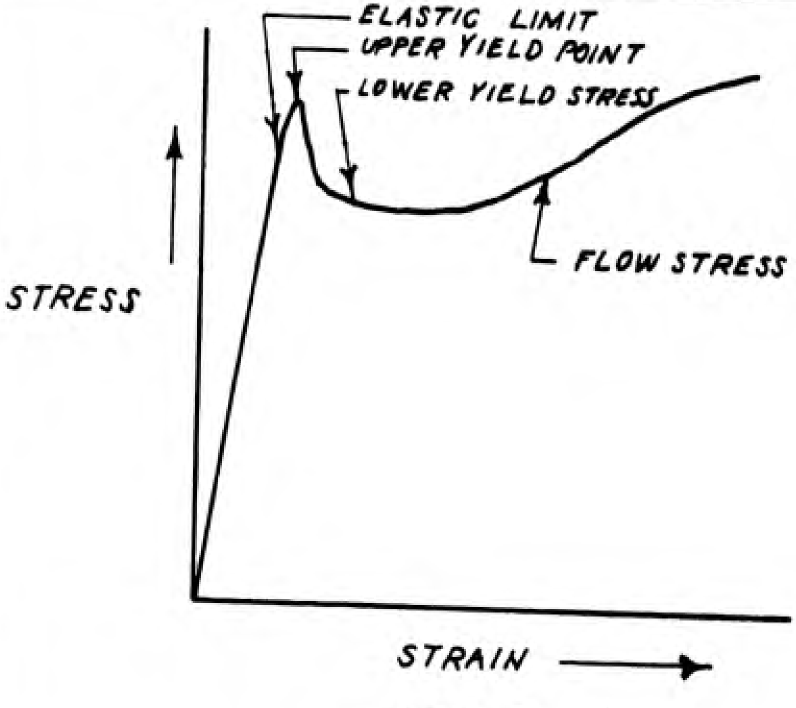

FIG. 8

PARTS OF A STRESS STRAIN CURVE

Fig. 9

Instron Testing Machine

The segment of the curve having the lower value of yield is called the lower yield stress, and the segment showing a rise in stress during strain hardening is called the flow stress, or flow curve.

If the material is unloaded after plastic deformation has occurred, and immediately reloaded, there is no yield point, or discontinuity, in the stress-strain curve. If the material is not reloaded after plastic deformation, the process of strain aging occurs as a function of temperature and time. After sufficient aging, there is a strengthening, or raising, of the flow curve, and a reappearance of the yield point (Ref 8:361).

Specimen History

Twelve tensile specimens were prepared from commercial-purity, powder-metallurgy, molybdenum sheet, 0.008 inch thick. The specimens were cut to size and recrystallized at 1204°C (2200°F) for one hour in a vacuum annealing furnace by the Metals and Ceramics Laboratory. Photomicrographs of the specimens, included in Appendix B, indicate that some of the specimens were not completely recrystallized.

Description of Tensile Testing Equipment

The tensile testing was done on an Instron testing machine such as shown in Figure 9. A "D" load cell was used with the full load scale set for 200 pounds. The crosshead speed was 0.020 inch per minute, and the chart speed was two inches per minute. The crosshead was set to return to a one and a half inch jaw separation. The machine was not calibrated to record strain. Instead, a load-elongation curve was autographically recorded.

Procedure

The specimens, shown in Figure 10, were given an initial plastic strain to a point where the flow curve begins to rise. The nominal load for the upper yield point was 130 pounds (approximately 65,000 psi).

The specimens were aged at selected temperatures until a yield was again observed. The aging temperatures, which ranged from 443°C to 580°C, were selected to give yield return times from 10 to 160 minutes. A drop of one pound (approximately 500 psi) in the load-elongation curve was sufficient to indicate the yield point return. The times for yield point return were found to be: 580°C, 11 minutes; 521°C, 28 minutes; 494°C, 50 minutes; 468°C, 85 minutes; and 443°C, 158 minutes.

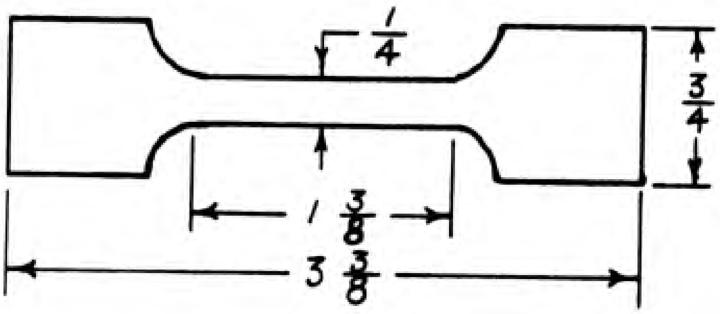

FIG. 10
TENSILE SPECIMEN FOR RETURN OF YIELD

Figure 11 gives a representative set of curves showing typical load-elongation behavior from initial yielding through yield point return.

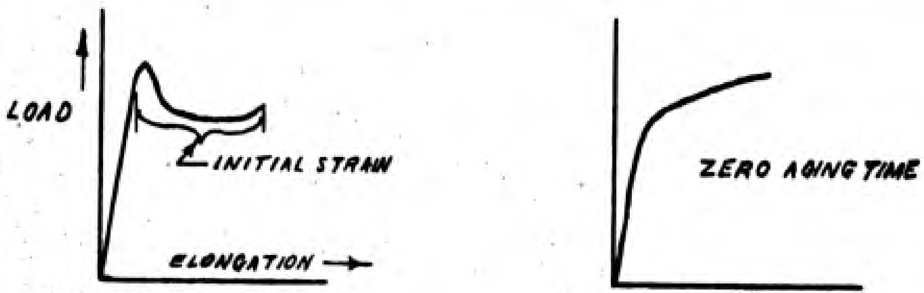

(a) INITIAL LOAD

(b) IMMEDIATE RELOAD

(C) INTERMEDIATE AGING

(d) Y.P. AGAIN OBSERVED

FIG. 11

TYPICAL LOAD-ELONGATION CURVES

Curve (a) displays the initial loading with its resultant sharp upper yield point and lower yield curve. Curve (b) shows immediate reloading, representing zero aging time, and (c) and (d) show the progression to return.

Originally, it was planned to use two samples for each aging temperature. It was soon discovered that some of the samples would not show a yield point return even though they were aged much longer than the expected time. This was attributed to incomplete recrystallization and possible variations in specimen chemistry. To offset this, more than one specimen was aged at the same time and these same specimens were used again at other temperatures. The specimens could be reused provided they were prestrained and no necking had occurred. In this way, any variation among specimens in aging time required for yield return could be averaged to a representative time. As it turned out, the unreliable specimens became evident immediately through group aging, and were discarded. A yield point return was obtained for enough specimens to give a reliable plot of the return rate.

As soon as a set of specimens giving consistent results was obtained, it was an easy matter to pinpoint the time for yield point return very closely. For example, the expected time for the lowest temperature, 443°C, was on the order of 150 minutes based on previous times obtained. Eight specimens were used. The first was aged for five minutes and quenched; the second was added to it and both placed in the aging bath for another five minutes and then quenched; this was repeated until all specimens had been placed in the bath with a five-minute aging time difference between each successive specimen. The specimens were all removed from the bath when the aging time varied from 135 to 170 minutes. Starting with the longest time, the specimen was checked for yield. If there was no yield, all the specimens with less time would be checked until the yield did not appear. The specimens with less time and no yield would be aged longer, but at closer time intervals, to pinpoint the time more accurately. By using this method, much time was saved.

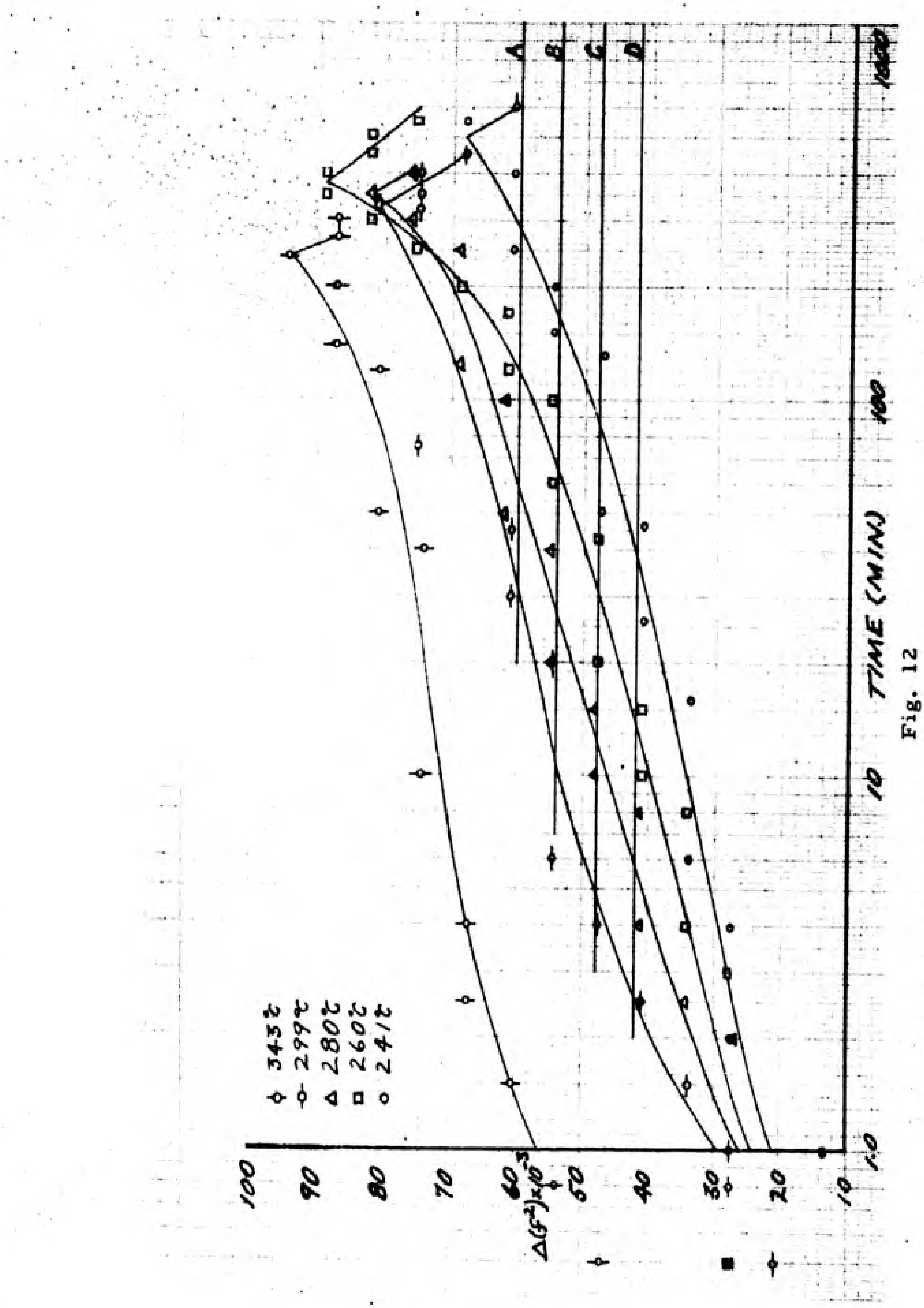

Fig. 12

Recovery of the Square of Resonant Frequency, as a Function of Aging Time and Temperature, After 3% Deformation by Compression

IV. Presentation and Discussion of Results

In both methods, the activation energy for strain aging was determined by plotting $\ln(\frac{1}{t})$ versus $\frac{1}{RT}$. Only one value of activation energy can be obtained from the yield point return data, but a range of values can be obtained from the dynamic modulus data by choosing different values of $\Delta(f^2)$, as shown in Figure 12 and explained on page 23.

Results of Modulus Recovery

The family of $\Delta(f^2)$ versus time curves for various aging temperatures is shown in Figure 12. Each curve exhibits an aging peak and then drops off to a lower value which appears to remain constant.

Each specimen was overaged from one to two hours to determine if any further decrease occurred. None was observed. This effect was also shown in the work of Wilcox (Ref 14:297-298, 302). He attributed the phenomenon to the coalescence, or growing together, of fine precipitates in the regions of dislocations. This caused an overaging effect with its inherent reduction in strength. The theory is that more interstitial atoms are attracted to the dislocations than can be retained in solid solution. The excess atoms interact with one another to form fine precipitates which add to the locking of the dislocations (Ref 7:6). As a result of overaging, the strengthening effect contributed by the precipitates is diminished.

It became evident that above approximately 300°C reliable data for determining the activation energy of interstitial diffusion could no longer be obtained. For this reason, the data taken at 388°C were omitted, but the data taken at 343°C were included to show the variation from the curves for lower temperatures. At temperatures above 300°C, the rate of modulus recovery was too fast to obtain a linear relation for determining activation energy.

To get the rate of return of the modulus, four horizontal lines,

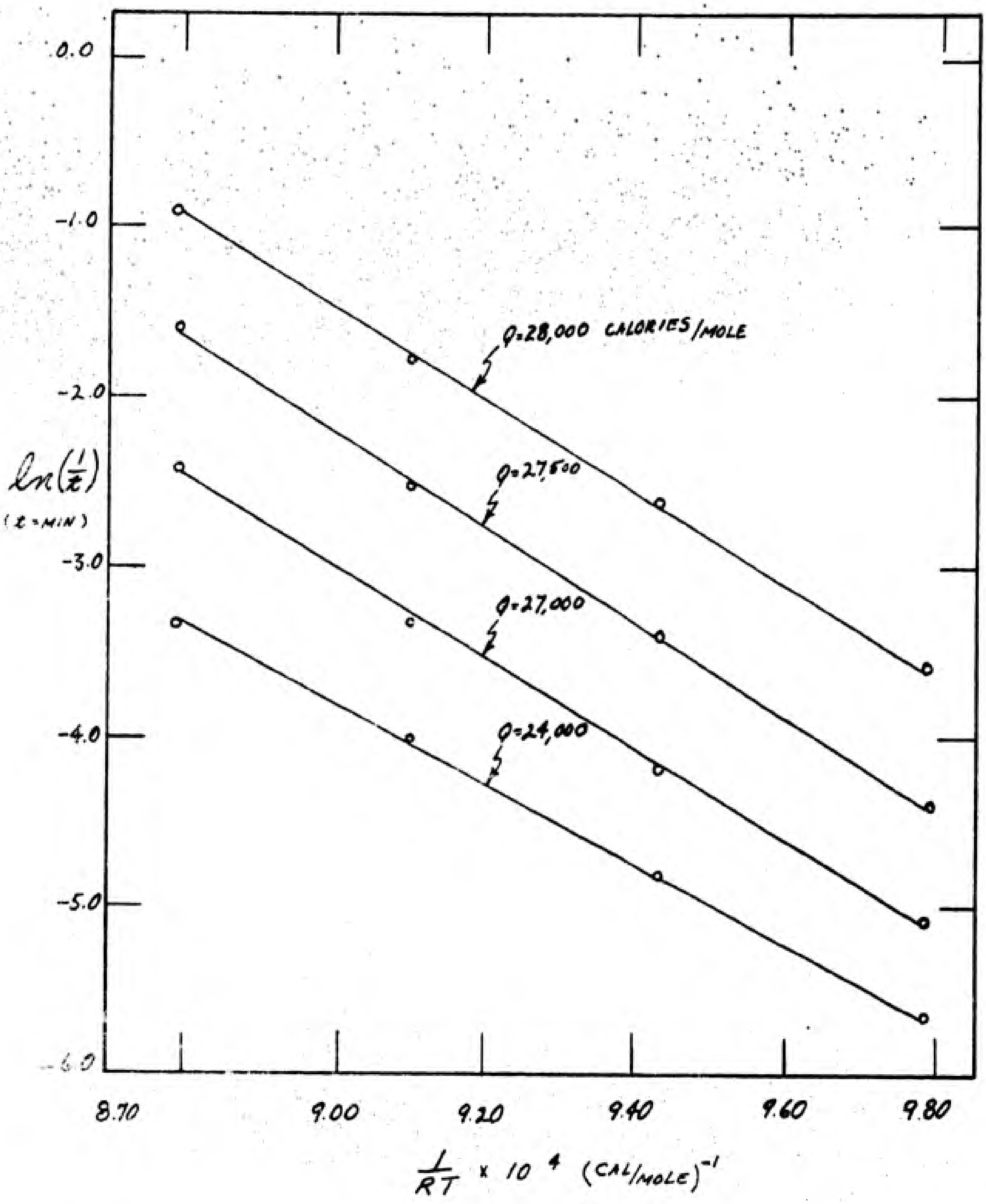

Fig. 13

Activation Energies Determined by Dynamic Modulus Method representing constant values of $\Delta(f^2)$, were drawn as shown in Figure 12, A, B, C, and D. The values of time and temperature at the intersections of the lines and curves were used to plot Figure 13. Four lines, of slope Q, corresponding to A, B, C, and D of Figure 12 were obtained. Their slope values for the activation energy of diffusion, of the as yet undetermined interstitial element, range from 24,000 to 28,000 calories per mole.

The effect of 3% deformation and subsequent strain aging on the modulus is shown in Table II. The Table lists values of E prior to deformation, after deformation, and at maximum recovery. In all specimens, the deformation caused a drop in Young's modulus of approximately 1.0×10^6 psi to 1.5×10^6 psi. Strain aging accounted for a recovery of about 350,000 psi. In terms of resonant frequency, deformation caused a drop of 120 - 150 cycles per second, of which 10 - 15 cycles per second were recovered. The difference between the number

Table II

Effect of 3% Deformation and Subsequent Strain Aging on the Dynamic Modulus for Flexural Vibration

E, Modulus of Undeformed Specimen	Eo, Modulus After Deformation (zero aging time)	Em, Modulus at Max. Recovery	Temp. °C
47.277×10^6 psi	46.517×10^6 psi	46.906×10^6 psi	343
47.779 "	46.270 "	46.598 "	299
48.164 "	47.026 "	47.355 "	280
48.515 "	47.400 "	47.761 "	260
47.825 "	46.535 "	46.810 "	241

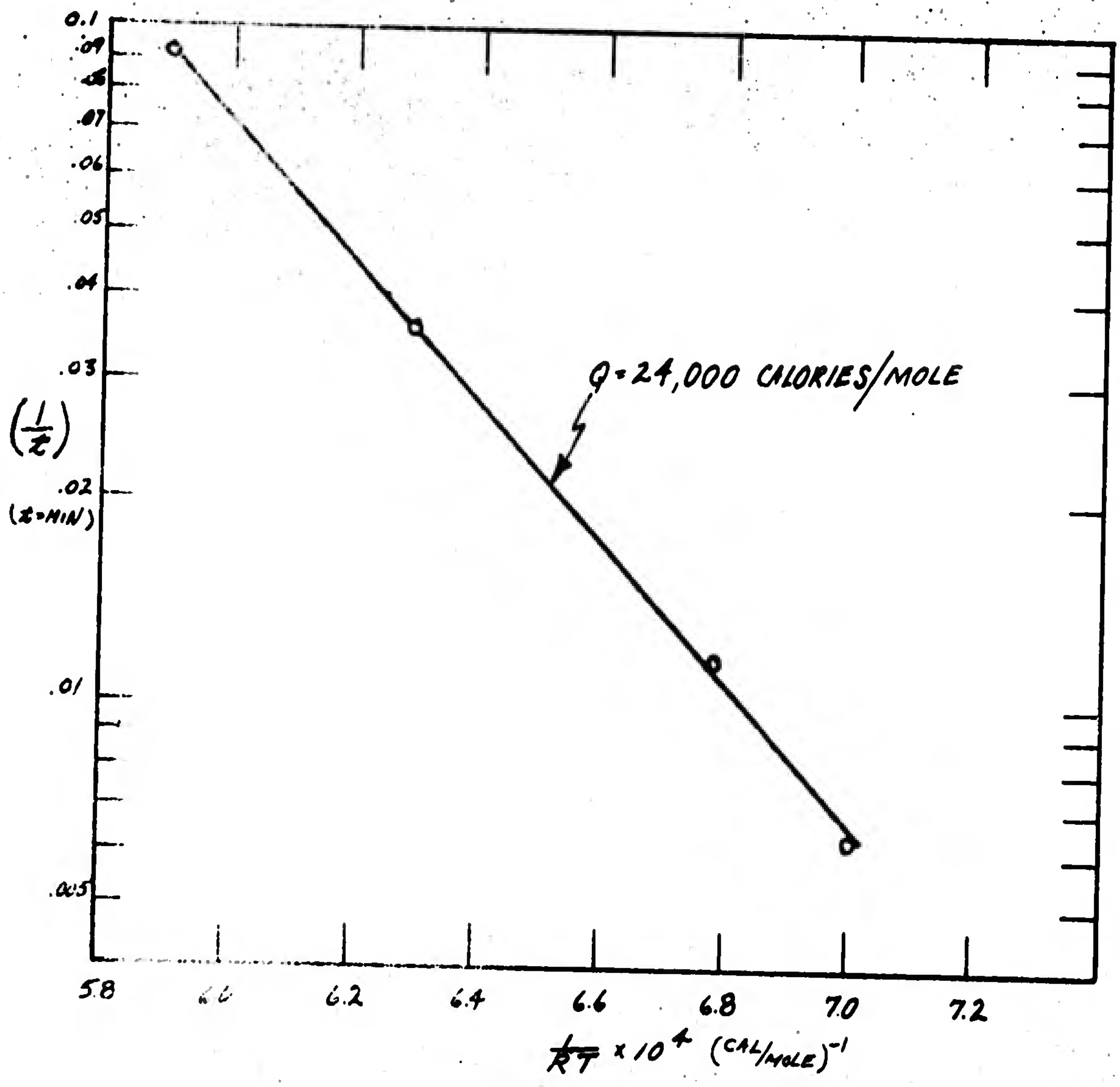

Fig. 14

Activation Energy Determined by Yield Point Return Method of cycles recovered by strain aging, and the total drop after deformation, can be accounted for by the change in thickness of the beam in flexure, and a change in the internal structure caused by deformation. The metal would have to be recrystallized to regain the value of E before deformation.

Results of Yield Point Return

The rate of return of the yield point is shown in Figure 14, where the reciprocal of the time for reappearance of the yield discontinuity is plotted against $\frac{1}{RT}$. The data for the graph are listed in Table III. The recorded load-elongation curves from which the times and temperatures were obtained have been placed in Appendix C.

Table III

Time of Yield Point Return For Each Aging Temperature

Recorded Values			Calculated Values	
Temperature °C	°K	Time (t) (Min)	$\frac{1}{RT*}$	$\ln(\frac{1}{t})$
443	716	158	7.02×10^{-4}	-5.05
468	741	85	6.78×10^{-4}	-4.44
494	767	50	6.55×10^{-4}	-3.91
521	794	28	6.31×10^{-4}	-3.40
580	853	11	5.89×10^{-4}	-2.49

*R = 1.99 cal/mole °K

The slope of the line in Figure 14 gives an activation energy of 24,000 calories per mole. As in the case of modulus recovery, it was found that there was a temperature limit above which the data no longer gave a linear relationship. Above 580°C the data were scattered and gave a much steeper slope. This indicated that the high temperature had provided enough thermal energy to activate another mechanism simultaneously with interstitial diffusion. Two mechanisms that could occur above this temperature are the beginning of self-diffusion, and the simultaneous movement of dislocations and interstitial atoms.

At the high temperature end of the straight line in Figure 14, a load drop of one pound (500 psi) was more critical than for lower temperatures. For example, one specimen indicated approximately a one pound yield for aging times of six minutes and four minutes at the same temperature. The time for yield point return would have to be called the shorter time which has the effect of increasing the slope of the straight line and the value of the activation energy.

Discussion

At sufficiently low temperatures, the process of strain aging, or the movement of interstitial atoms back to the dislocations lines, is controlled by the diffusion rate. Therefore, the activation energy for strain aging should be in close agreement with that for interstitial diffusion (Ref 7:7). At present, there is insufficient data on the activation energies for diffusion of interstitial elements in molybdenum to make a comparison with the energies obtained by this investigation. The available data for diffusion in refractory metals are compiled in a recent report by Peterson (Ref 10:57). Values of interest for diffusion of carbon, hydrogen, nitrogen, and oxygen in molybdenum are as follows:

C	(1200 - 2000°C)	33,400 cal/mole ± 10,300 (Samsonov and Latysheva)
H	(575 - 980°C)	14,700 cal/mole (Hill)
N	(1100 - 1600°C)	45,000 cal/mole (Smithells and Ransky) 53,000 cal/mole (Maringer and Muehlenkamf)
O	No data available	

When compared to the above data, the activation energies determined during this investigation indicate that hydrogen and nitrogen are not the interstitial elements responsible for the strain aging in molybdenum; hydrogen being too low, and nitrogen too high. This leaves a choice between carbon and oxygen.

Due to lack of time, it was not feasible to analyze the tensile specimens for interstitial content. A typical analysis of commercial-purity molybdenum gives the following interstitial content (Ref 6:27):

Element	Parts per Million
Oxygen	10 - 100
Carbon	10 - 400
Nitrogen	8 - 80

The amount of hydrogen is usually reported as a trace.

The modulus specimens were analyzed by the General Electric Laboratory to give the following content:

Element	Parts per Million (by weight)
Oxygen	10
Carbon	30
Nitrogen	4
Hydrogen	less than 1

This indicates better than commercial purity for the modulus specimens. Previous investigations of strain aging in other metals indicate that the amounts of carbon and oxygen present in these molybdenum specimens are sufficient to cause the observed strain aging (Ref 7:16, 20, 27).

V. Conclusions

The activation energies of 24,000 calories per mole for yield point return and 24,000 to 28,000 calories per mole for dynamic modulus recovery are in good agreement. A comparison of these activation energies with the available data for interstitial diffusion in molybdenum indicates that either carbon or oxygen is responsible for strain aging in molybdenum.

In both methods of determining an activation energy, an upper temperature limit was found. Above these temperatures, the rate processes occurred too fast to give a linear relation on a plot of $\ln(\frac{1}{t})$ versus $\frac{1}{RT}$. To get good values of activation energy, it is necessary to obtain sufficient data at temperatures well below the limit to establish the linear relationship for the rate process. For the method of yield point return, the straight line should be established for times longer than twenty minutes to give a reliable value of activation energy.

VI. Recommendations for Future Work

A logical continuation of this investigation would be to find a method for the determination of the interstitial element responsible for strain aging. Internal friction measurements may hold some promise since both activation energy and alloy content are determined. An alloying element has the effect of lowering the height of the internal-friction peak of the pure metal and producing at a higher temperature, a second peak, whose height is a function of the amount of alloy in solution. At low concentrations of solute, the alloy peak is not distinct, and the activation energies cannot be calculated (Ref 1:232-233). This imposes a limit on the use of internal friction methods with molybdenum since the solid solubilities of carbon and oxygen are very low. The solubilities of carbon, oxygen, and nitrogen in molybdenum are shown in Figure 15. The diagrams are based on existing metallographic, ductile-to-brittle transition temperature, and chemical data obtained from several sources. Commercial wrought molybdenum usually contains more carbon, oxygen, and nitrogen than are soluble at room temperature.

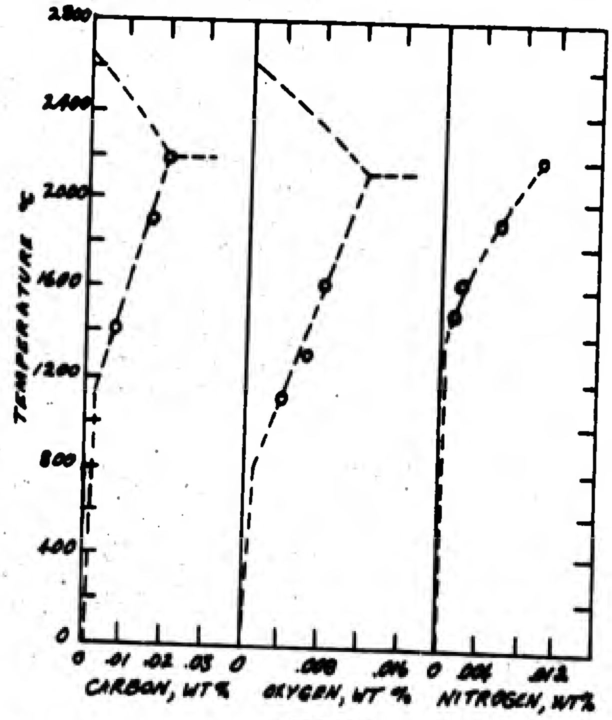

FIG. 15

TENTATIVE DIAGRAMS TO ILLUSTRATE SOLID SOLUBILITY OF CARBON, OXYGEN, AND NITROGEN IN MOLYBDENUM

(Ref 12:267)

Another method which holds more promise is to dose single crystals with interstitials, and take measurements of various properties to determine activation energies. Some of this work is being done by M. A. Adams of the Materials Research Corporation, Yonkers, New York. He is dosing single crystals of molybdenum with one interstitial element at a time, and taking yield point return data to determine the activation energy for interstitial diffusion.

List of References

1. Conrad, Hans, "The Role of Grain Boundaries In Creep and Stress Rupture," in Mechanical Behavior of Materials at Elevated Temperatures, edited by J. E. Dorn. New York: McGraw-Hill Book Co., Inc. 1961, pp. 218-269.

2. Cottrell, A. H. "Effect of Solute Atoms on the Behavior of Dislocations," Report of a Conference on the Strength of Solids. The Physical Society, London, 1948, pp. 30-37.

3. Ferro, A. "Theory of Diffusion Constants in Interstitial Solid Solutions of b.c.c. Metals." Journal of Applied Physics, 28: 895-900 (August, 1957).

4. Guy, A. G. Elements of Physical Metallurgy (Second Edition). Reading, Mass., Addison-Wesley Pub. Co., 1959.

5. Hasselman, D. P. H. Tables for the Computation of the Shear Modulus and Young's Modulus of Elasticity from the Resonant Frequencies of Rectangular Prisms. Niagara Falls, New York: Carborundum Co., Unpublished Report, 1961.

6. Houck, J. A. Physical and Mechanical Properties of Commercial Molybdenum-Base Alloys. DMIC Report 140. Columbus, Ohio: Battelle Memorial Institute, November 30, 1960.

7. Imgram, A. G. Strain Aging of Refractory Metals. DMIC Report 134. Columbus, Ohio: Battelle Memorial Institute, August 12, 1960.

8. Lubahn, J. D. "Deformation Phenomena," in Mechanical Behavior of Materials at Elevated Temperatures, edited by J. E. Dorn. New York: McGraw-Hill Book Co., Inc., 1961 pp. 319-392.

9. Maringer, R. E., and Schwope, A. D. "The Anelasticity of Molybdenum," Sixteenth Quarterly Report to Office of Naval Research, Contract No. NOnr 82100, Battelle Memorial Institute, July 14, 1953.

10. Peterson, N. L. Diffusion in Refractory Metals. WADD Technical Report 60-793. WP-AFB, Dayton, Ohio: Wright Air Development Division, March 1961.

List of References

11. Richards, J. T. "An Evaluation of Several States and Dynamic Methods for Determining Elastic Moduli," Symposium on Determination of Elastic Constants, New York: American Society for Testing Materials, 1952, pp. 71-98.

12. Spacil, H. S., and Wulff, J. "Effects of Oxygen, Nitrogen, and Carbon on the Ductility of Wrought Molybdenum," in The Metal Molybdenum, edited by J. J. Harwood. Cleveland, Ohio: American Society for Metals, 1958, pp. 262-280.

13. Toensing, C. H. "Molybdenum Metal Powder," in The Metal Molybdenum, edited by J. J. Harwood. Cleveland, Ohio: American Society for Metals, 1958, pp. 31-50.

14. Wilcox, B. A., and Huggins, R. A. "Effect of Hydrogen on Dislocation Locking in Niobium," Journal of the Less-Common Metals, 2: 292-303 (August 1960).

Appendix A

Modulus Data

Specimen #7 241°C (466°F)

Cumulative Aging Time (min)	Frequency c/s	f^2	$(f_t^2 - f_o^2)$ $\Delta(f^2)$
Undeformed	3552	12,616,704	
Deformed (f_o)	3397	11,539,609	
1	3399	11,553,201	13,592
2	3401	11,566,801	27,192
3	01	"	"
4	01	"	"
6	3402	11,573,604	33,995
11	02	"	"
16	02	"	"
26	3403	11,580,409	40,800
36	03	"	"
41	03	"	"
46	03	"	"
51	3404	11,587,216	47,607
71	04	"	"
91	04	"	"
101	04	"	"
111	04	"	"
121	04	"	"
131	04	"	"
151	3405	11,594,025	54,416
200	05	"	"
250	3406	11,600,836	61,227
300	06	"	"
350	06	"	"
400	06	"	"
450	3407	11,607,649	68,040
470	07	"	"
500	07	"	"
550	07	"	"
600	3406	11,600,836	61,227

Appendix A

Modulus Data

Specimen #6 260°C (500°F)

Cumulative Aging Time (min)	Frequency c/s	f^2	$(f_t^2 - f_o^2)$ $\Delta(f^2)$
Undeformed	3553	12,623,809	
Deformed (f_o)	3417	11,675,889	
0.5	3421	11,703,241	27,352
1	21	"	"
2	21	"	"
3	21	"	"
4	3422	11,710,084	34,195
5	22	"	"
7	22	"	"
10	3423	11,716,929	41,040
15	23	"	"
20	3424	11,723,776	47,887
30	24	"	"
40	24	"	"
42	24	"	"
50	3425	11,730,625	54,736
75	25	"	"
100	25	"	"
120	3426	11,737,476	61,587
140	26	"	"
170	26	"	"
200	3427	11,744,329	68,440
250	3428	11,751,184	75,295
300	3429	11,758,041	82,152
350	3430	11,764,900	89,011
400	30	"	"
450	3429	11,758,041	82,152
500	29	"	"
550	3428	11,751,184	75,295

Appendix A

Modulus Data

Specimen #8 280°C (536°F)

Cumulative Aging Time (min)	Frequency c/s	f^2	$(f_t^2 - f_o^2)$ $\Delta(f^2)$
Undeformed	3560	12,673,600	
Deformed (f_o)	3438	11,819,844	
0.5	3442	11,847,364	27,520
1.5	42	"	"
2.0	42	"	"
2.5	3443	11,854,249	34,405
4.0	3444	11,861,136	41,292
5.0	44	"	"
8.0	44	"	"
10	3445	11,868,025	48,181
15	45	"	"
20	3446	11,874,916	55,072
30	46	"	"
40	46	"	"
50	3447	11,881,809	61,965
60	47	"	"
75	47	"	"
100	47	"	"
125	3448	11,888,704	68,860
150	48	"	"
175	48	"	"
200	48	"	"
250	48	"	"
300	3449	11,895,601	75,757
350	3450	11,902,500	82,656
400	3449	11,895,601	75,757

Appendix A

Modulus Data

Specimen #1 299°C (570°F)

Cumulative Aging Time (min)	Frequency c/s	f^2	$f_t^2 - f_o^2$ $\Delta(f^2)$
Undeformed	3548	12,588,304	
Deformed (f_o)	3395	11,526,025	
0.5	3398	11,546,404	20,379
0.8	3399	11,553,201	27,176
1.0	99	"	"
1.5	3400	11,560,000	33,975
2.5	3401	11,566,801	40,776
4.0	3402	11,573,604	47,579
6.0	3403	11,580,409	54,384
8	03	"	"
10	03	"	"
15	03	"	"
20	03	"	"
30	3404	11,587,216	61,191
40	04	"	"
50	3405	11,594,025	68,000
75	3406	11,600,836	74,811
100	06	"	"
120	06	"	"
140	06	"	"
160	06	"	"
200	06	"	"
240	06	"	"
300	06	"	"
320	06	"	"
330	3407	11,607,649	81,624
340	07	"	"
350	3406	11,600,836	74,811
400	06	"	"
450	3405	11,594,025	68,000

Appendix A

Modulus Data

Specimen #3 343°C (650°F)

Cumulative Aging Time (min)	Frequency c/s	f^2	$(f_t^2 - f_o^2)$ $\Delta(f^2)$
Undeformed	3503	12,271,009	
Deformed (f_o)	3357	11,269,449	
0.5	3364	11,316,496	47,047
0.9	3365	11,323,225	53,776
1.5	3366	11,329,956	60,507
2.5	3367	11,336,689	67,240
4.0	67	"	"
10	3368	11,343,424	73,975
15	68	"	"
20	68	"	"
30	68	"	"
40	68	"	"
50	3369	11,350,161	80,712
75	69	"	"
100	69	"	"
120	69	"	"
140	3370	11,356,900	87,451
160	70	"	"
180	70	"	"
200	70	"	"
240	3371	11,363,641	94,192
270	3370	11,356,900	87,451
305	70	"	"

Appendix B

Photomicrographs of Tensile Specimens

Bausch and Lomb Metallograph, Eyepiece 10x, 250 Magnification

Electropolish, 3 volts, 50 seconds; Etch, 10g $Fe(CN)_6$. 10g KOH 100g H_2O

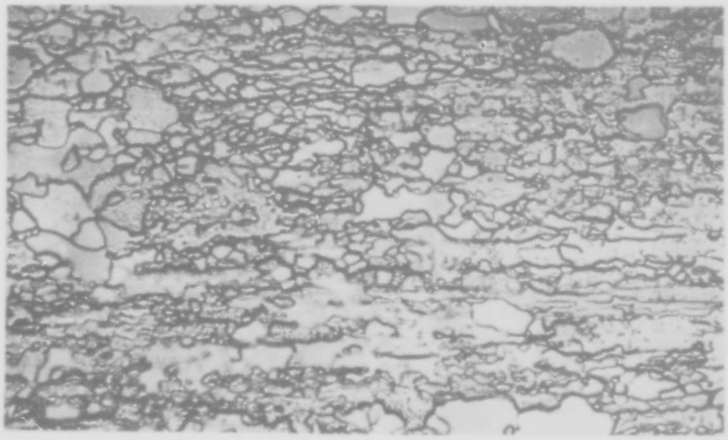

SPECIMEN #1

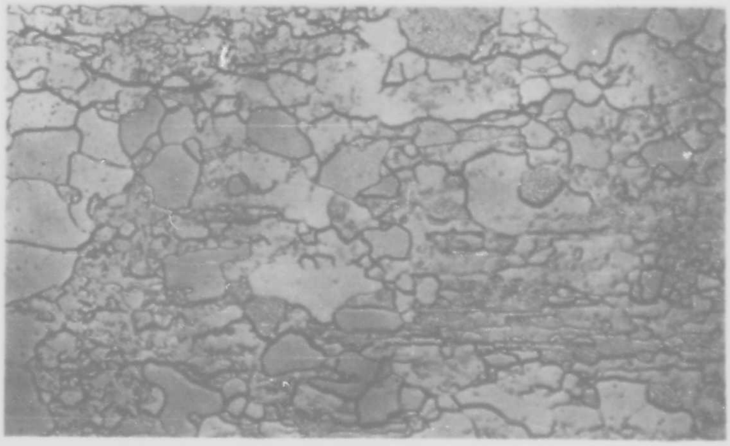

SPECIMEN #2

Appendix B

Photomicrographs of Tensile Specimens

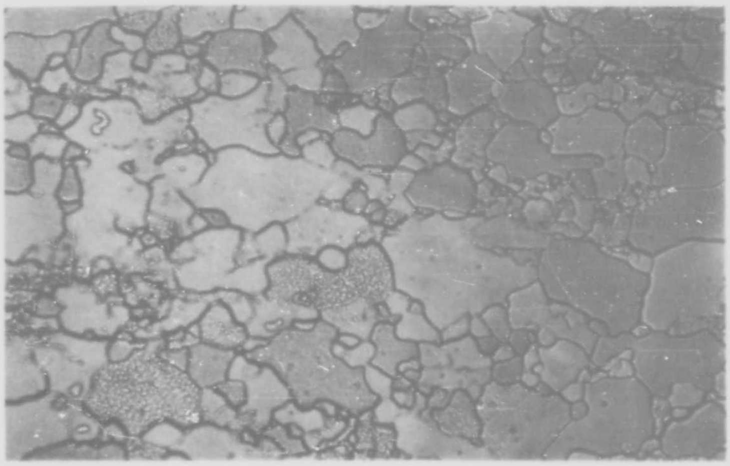

SPECIMEN #3

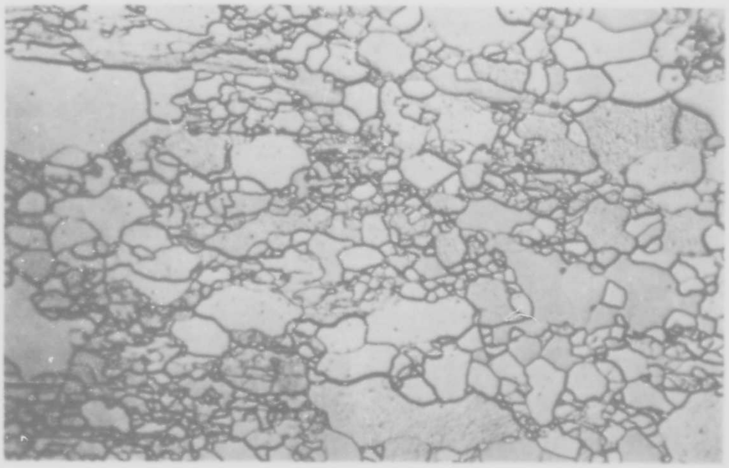

SPECIMEN #4

Appendix B

Photomicrographs of Tensile Specimens

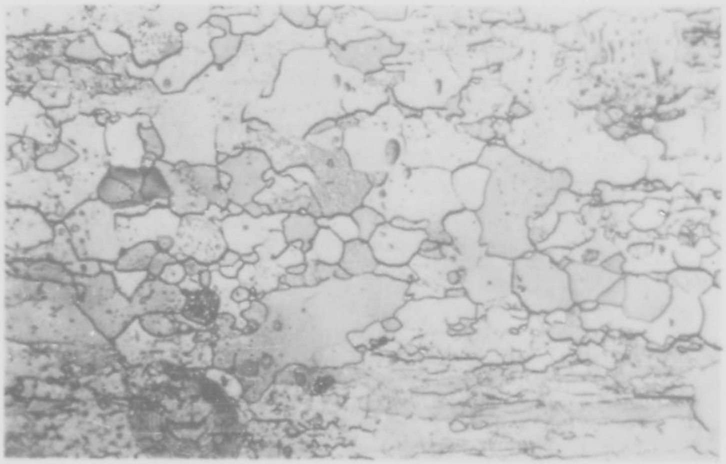

SPECIMEN #5

SPECIMEN #6

Appendix B

Photomicrographs of Tensile Specimens

SPECIMEN #7

SPECIMEN #8

Appendix C

Load-Elongation Curves

Chart speed, 2 inches/minute; Crosshead speed, 0.020 inch/minute

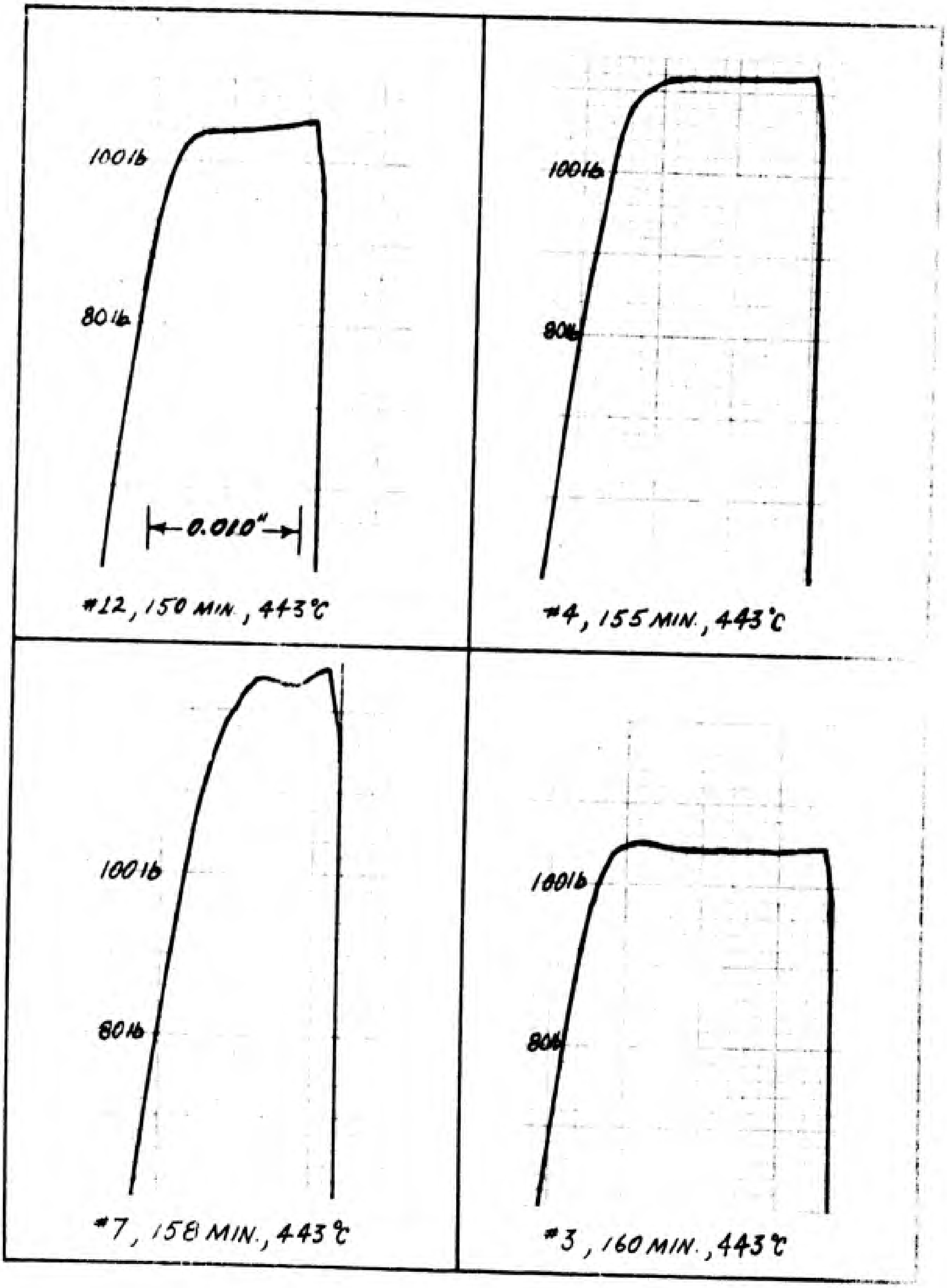

#12, 150 MIN, 443°C

#4, 155 MIN., 443°C

#7, 158 MIN., 443°C

#3, 160 MIN., 443°C

Appendix C

Load-Elongation Curves

Chart speed, 2 inches/minute; Crosshead speed, 0.020 inch/minute

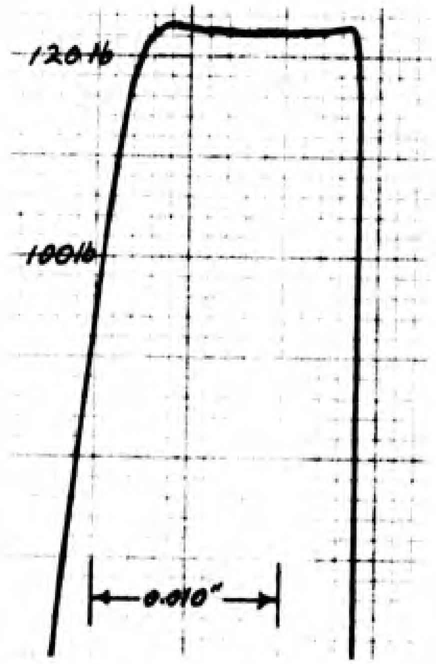

#7, 85 MIN., 468°C

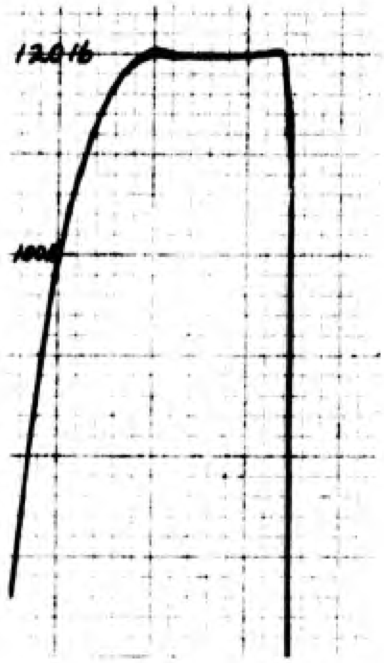

#6, 28 MIN., 521°C

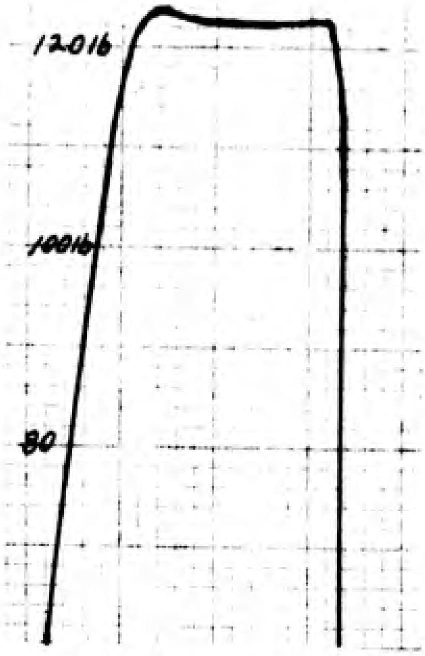

#7, 30 MIN., 521°C

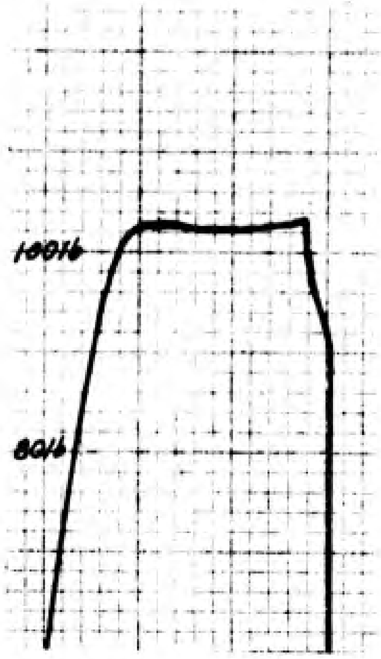

#4, 31 MIN., 521°C

Appendix C

Load-Elongation Curves

Chart speed, 2 inches/minute; Crosshead speed, 0.020 inch/minute

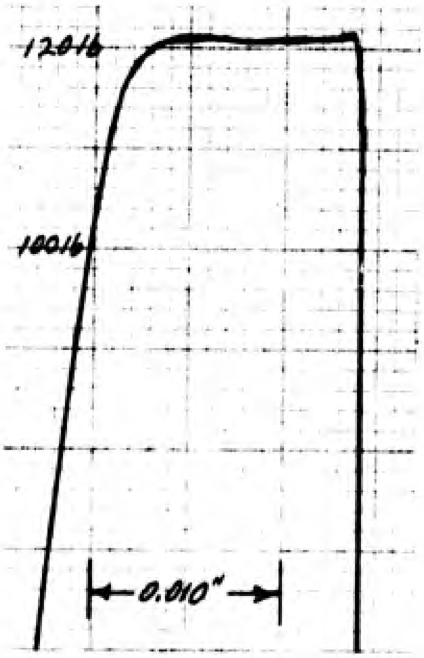

#6, 11 MIN., 580°C

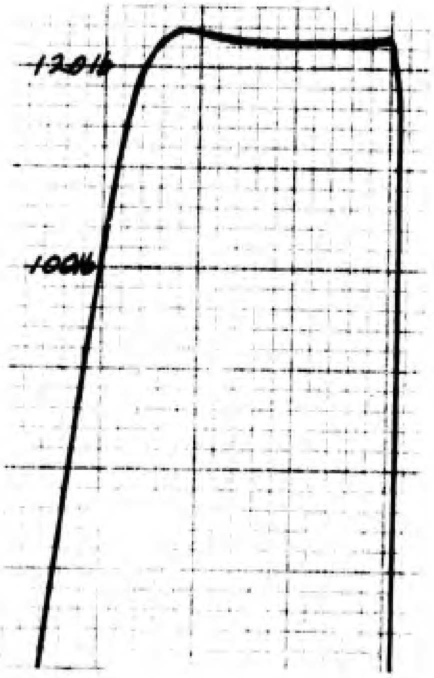

#7, 12 MIN., 580°C

#3, 13 MIN., 580°C

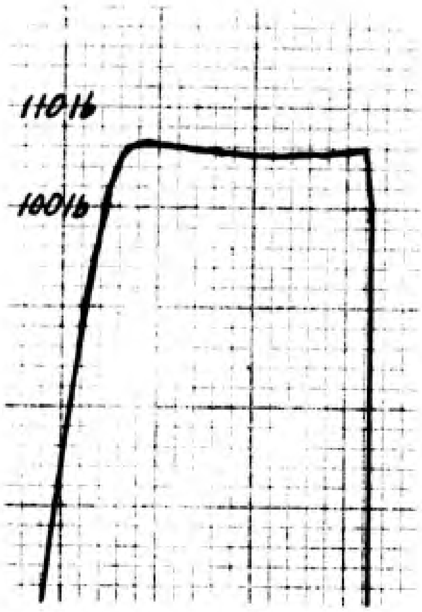

#4, 13 MIN., 580°C

Appendix C

Load-Elongation Curves

Chart speed, 2 inches/minute; Crosshead speed, 0.020 inch/minute

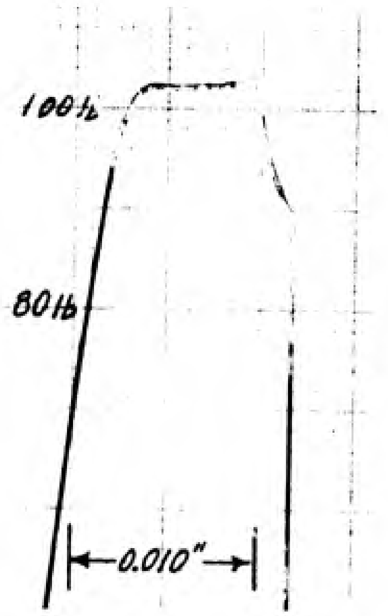

#4, 45 MIN., 494°C

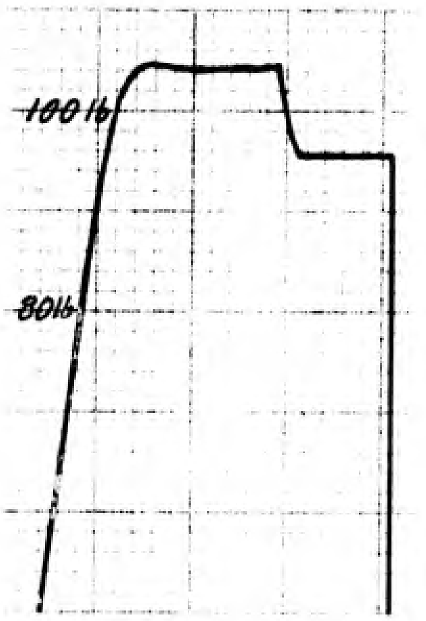

#3, 50 MIN., 494°C

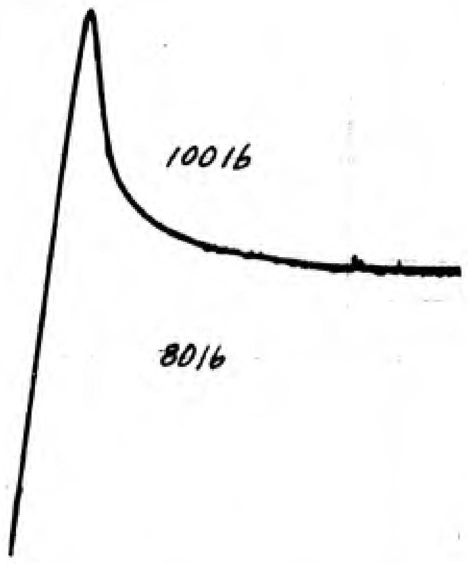

#3, INITIAL YIELD

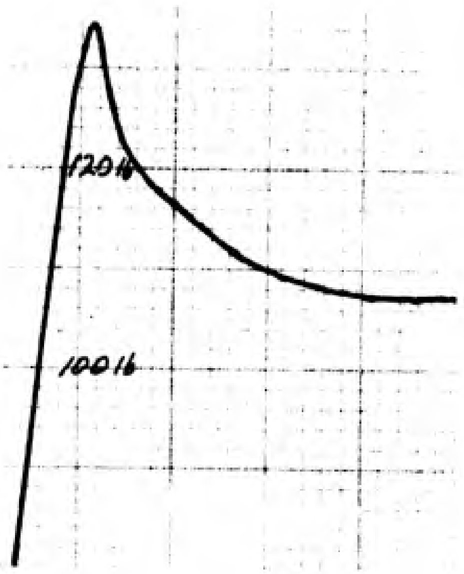

#7, INITIAL YIELD

Vita

Robert John Wilson was born on [redacted], [redacted], the son of Raymond Wilbur Wilson and Adeline [redacted] Wilson. After graduating from [redacted], he worked in a variety of jobs until entering trade school to study turret lathe operation. Completing this in late 1940, he worked throughout 1941 setting up and operating turret lathes. He entered the U. S. Army Air Corps in January 1942, served overseas as a fighter pilot in China during 1943 and 1944 and was separated from the service in 1946. From 1946 through 1951, he worked as a machinist and sales engineer and was accepted as a union journeyman carpenter after completion of apprenticeship and examination. During this same period he attended a night course in mechanical engineering at the Bridgeport Engineering Institute, Bridgeport, Connecticut and received a diploma in 1951. He was recalled to active duty in October 1951, completed undergraduate electrical engineering at the Air Force Institute of Technology in 1955, and served as a Research and Development Staff Officer with the Electronics Directorate at the Cambridge Research Center, Bedford, Massachusetts until his reassignment to the Institute of Technology.

Permanent address: [redacted]

UNCLASSIFIED

UNCLASSIFIED